

# Stochastic resonance without tuning

J. J. Collins\*<sup>†</sup>, Carson C. Chow\*  
& Thomas T. Imhoff\*

\* NeuroMuscular Research Center, <sup>†</sup> Department of Biomedical Engineering, Boston University, 44 Cummings Street, Boston, Massachusetts 02215, USA

STOCHASTIC resonance<sup>1-4</sup> (SR) is a phenomenon wherein the response of a nonlinear system to a weak periodic input signal is optimized by the presence of a particular, non-zero level of noise<sup>5-7</sup>. SR has been proposed as a means for improving signal detection in a wide variety of systems, including superconducting quantum interference devices<sup>8</sup>, and may be used in some natural systems such as sensory neurons<sup>9-15</sup>. But for SR to be effective in a single-unit system (such as a sensory neuron or a single ion channel), the optimal intensity of the noise must be adjusted as the nature of the signal to be detected changes<sup>15</sup>. This has been thought to impose a limitation on the practical and natural uses of SR. Here we show that the ability of a summing network of excitable units to detect a range of weak (sub-threshold) signals (either periodic or aperiodic) can be optimized by a fixed level of noise, irrespective of the nature of the input signal. We also show that this noise does not significantly degrade the ability of the network to detect supra-threshold signals. Thus, large nonlinear networks do not suffer from the limitations of SR in single units, and might be able to use a single noise level, such as that provided by the intrinsic noise of the individual components, to enhance the system's sensitivity to weak inputs. This suggests a functional role for neuronal noise<sup>14,16-18</sup> in sensory systems.

We considered a summing network (Fig. 1) of identical excitable units, which were taken to be FitzHugh-Nagumo (FHN) model neurons (for details, see Fig. 1 legend). Each unit was subjected to a common input signal and its own independent noise source (which could be intrinsic or externally added to each unit). We assumed that information was transmitted by each unit via temporal changes in its firing rate. (This is a valid assumption for many types of sensory neurons<sup>19</sup>.) The network operated by summing the mean firing rate (MFR) signal from each unit to obtain a resultant MFR signal for the entire system (Fig. 1). The motivation for studying this system was twofold: (1) networks of this sort can be easily constructed and incorporated into signal-detection systems<sup>20</sup>, and (2) such networks are appropriate models for many neurophysiological sensory systems<sup>21</sup>.

Recently, it was shown that SR-type behaviour can be characterized in excitable systems with aperiodic inputs<sup>22</sup>. This general type of behaviour was termed aperiodic stochastic resonance (ASR). To characterize ASR in the summing network of Fig. 1, we considered the normalized power norm  $C_3$  given by

$$C_3 = \frac{S(t)R_\Sigma(t)}{[S^2(t)]^{1/2}[(R_\Sigma(t) - R_\Sigma(t))^{2}]^{1/2}} \quad (1)$$

where  $S(t)$  is an aperiodic (zero-mean) input signal (see Fig. 1 legend),  $R_\Sigma(t)$  is the resultant MFR signal for the network, and the overbar denotes an average over time. (For ASR, the exact form of  $S(t)$  is unimportant (it could be periodic, for example), provided that its variations occur on a timescale which is slower than the characteristic time(s) of the system under study<sup>22</sup>.) Maximizing  $C_3$  corresponds to maximizing the coherence between the input stimulus  $S(t)$  and the system response  $R_\Sigma(t)$ .

The numerical results for  $N$ -unit summing networks with a sub-threshold aperiodic input signal are given in Fig. 2. Shown are the values of  $C_3$  as a function of the input noise intensity  $D$ . (The solid curves are from the theory to be described below.) The

results for a single-unit ( $N=1$ ) network showed characteristic signatures of SR-type behaviour: a rapid rise to a clear peak, and then a slow decrease for higher values of  $D$ . As the number of units in the network was increased, the peak  $C_3$  value increased, that is, it asymptotically approached 1.0 (Fig. 2). Thus, the stimulus-response coherence was enhanced as the size of the network was increased. This finding is consistent with those of other studies which have considered conventional SR in uncoupled<sup>20</sup> and coupled<sup>23-30</sup> networks of nonlinear elements. In addition, and perhaps more importantly, as the size of the network was increased, the post-peak decay rate of  $C_3$  (relative to the ASR peak amplitude) diminished, that is,  $C_3$  asymptotically approached a plateau near 1.0 for a range of noise intensity values larger than the optimal value for a single unit (Fig. 2). This plateau indicates that for large  $N$ , maximum fidelity is attained for a wide range of noise values.

We have developed a theory<sup>22</sup> of ASR for a single excitable unit, based on the following dynamics of the FHN model. (Kiss *et al.*<sup>31,32</sup> independently developed a theory for SR-type behaviour in threshold devices with wideband input signals.) For a sub-threshold activation signal (see Fig. 1 legend), the FHN model has a stable fixed point. Input gaussian noise 'kicks' the system away from the fixed point. If the system is kicked over its threshold, it 'fires' and subsequently returns to the stable fixed point after a refractory period. To calculate the mean firing rate  $R_i(t)$ , which is proportional to the probability of escaping from the stable fixed point, we formulated the problem as a barrier-escape problem. We then used Kramers' formula for the escape rate<sup>33</sup> to derive the following expression for  $R_i(t)$ :

$$\langle R_i(t) \rangle \propto \exp(-\sqrt{3}[B^3 - 3B^2S(t)]\varepsilon/D) \quad (2)$$

where the angle brackets  $\langle \rangle$  denote an ensemble average,  $B$  is the signal-to-threshold distance (that is, the barrier height), and  $\varepsilon$  is an FHN model parameter (see Fig. 1 legend).

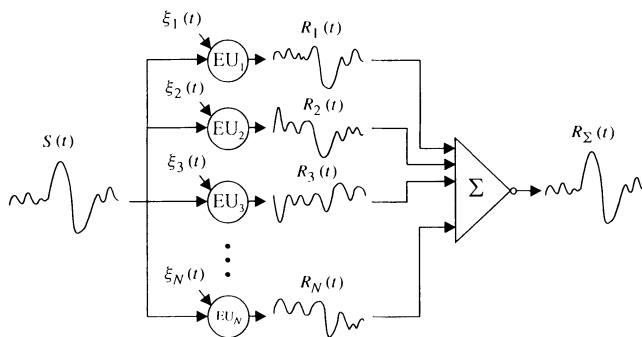


FIG. 1 A summing network of  $N$  excitable units ( $EU_i$ ). Each  $EU_i$  was a FitzHugh-Nagumo model neuron<sup>13</sup>, governed by the following equations:

$$\varepsilon \dot{v}_i = v_i(v_i - a)(1 - v_i) - w_i + A + S(t) + \xi_i(t),$$

$$\dot{w}_i = v_i - w_i - b$$

where  $v_i(t)$  is a fast (voltage) variable,  $w_i(t)$  is a slow (recovery) variable,  $A$  is a constant (tonic) activation signal,  $\varepsilon=0.005$ ,  $a=0.5$ ,  $b=0.15$ ,  $\xi_i(t)$  is unit-independent gaussian white noise with zero mean and auto-correlation  $\langle \xi_i(t)\xi_j(t_j) \rangle = 2D\delta(t-t_j)$ , the angle brackets  $\langle \rangle$  denote an ensemble average over the noise distribution,  $D$  is the noise intensity, and  $S(t)$  is a slowly varying aperiodic signal which was common to all units in the network. The time-varying mean firing rate (MFR) signal  $R_i(t)$  for each unit, was computed by passing a unit-area symmetric Hanning window filter<sup>34</sup> over an impulse train corresponding to the firings of each unit, which were determined using the method described in ref. 13. The summer ( $\Sigma$ ) operated by averaging the MFR signals from the respective units to obtain a resultant MFR signal  $R_\Sigma(t)$  for the network. Each unit's MFR signal was equally weighted by the summer. (In ref. 20, conventional SR was examined in a similar network of Schmitt triggers.)

This analysis can be extended to a summing network of  $N$  excitable units. To derive an expression for  $C_3$ , we need an expression for  $R_{\Sigma}(t)$ . We use the supposition that  $R_i(t)$  is equal to the ensemble average (given by equation (2)) plus a fluctuating term which arises from the input noise. It can then be shown that  $R_{\Sigma}(t)$  is equal to the same ensemble average plus a stochastic term which scales as  $N^{-1/2}$ . This rate expression can be substituted into equation (1) and with some algebraic manipulations and averaging operations, it can be shown that

$$C_3 = \frac{\Delta[\overline{S^2(t)}]^{1/2}}{[\exp(\Delta^2 \overline{S^2(t)}) - 1 + (\sigma^2(D)/N) \exp(2V/D) \exp(-\Delta^2 \overline{S^2(t)})]^{1/2}} \quad (3)$$

where  $\Delta = 3\sqrt{3}\varepsilon B^2/D$ ,  $V = \sqrt{3}\varepsilon B^3$  and  $\sigma^2(D)$  is an empirical function of  $D$  (ref. 22). From equation (3), it can be seen that the theory matches the numerical data (Fig. 2), predicting that as  $N$  increases,  $C_3$  asymptotically approaches a plateau near 1.0 for a range of noise intensity values larger than the optimal value for a single unit. (Note that it can be shown that equation (3) is unchanged for a summing network of non-identical excitable units, that is, ones with slightly different thresholds. The variation in  $B$  across the units of the network enhances the amplitude of  $R_{\Sigma}(t)$  by a constant factor, which is normalized out in the calculation of  $C_3$  (equation (1)).)

It can be shown from equation (3) that

$$N = \frac{aC_3^2}{1 - C_3^2} \quad (4)$$

where  $a = \sigma^2[(1 - \Delta^2 \overline{S^2(t)})/\Delta^2 \overline{S^2(t)}] \exp(2V/D)$ . Thus, for any  $D$  and  $\sigma^2$ , one can calculate the number of network units needed to obtain a desired level of fidelity.

The plateau in the  $C_3(D)$  curve (Fig. 2) of a relatively large (for example,  $N=1,000$ ) summing network suggests that a fixed

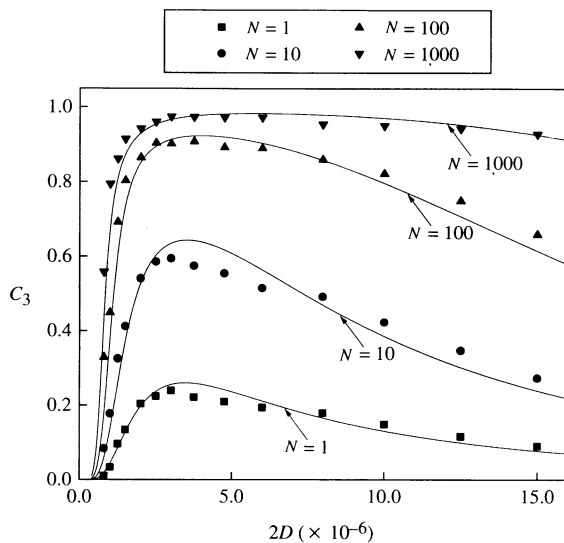


FIG. 2 Values (symbols) of the normalized power norm  $C_3$  plotted against  $2D$ , where  $D$  is the intensity of the input gaussian white noise on each unit, for  $N$ -unit summing networks with a sub-threshold aperiodic input signal  $S(t)$ . The theoretical predictions (solid curves) from equation (3) are also shown. The model equations for each unit (see Fig. 1 legend) were solved numerically using an algorithm developed for stochastic differential equations<sup>35</sup>. An integration stepsize of 0.001 s was used. The reported results did not change for smaller stepsizes.  $S(t)$  was formed by convolving gaussian correlated noise (with correlation time of 20 s) with the filter described in Fig. 1 legend. The same input signal  $S(t)$ , with variance of  $1.5 \times 10^{-5}$  and total time length of 300 s, was used for all results presented. The signal-to-threshold distance  $B$  was 0.07.

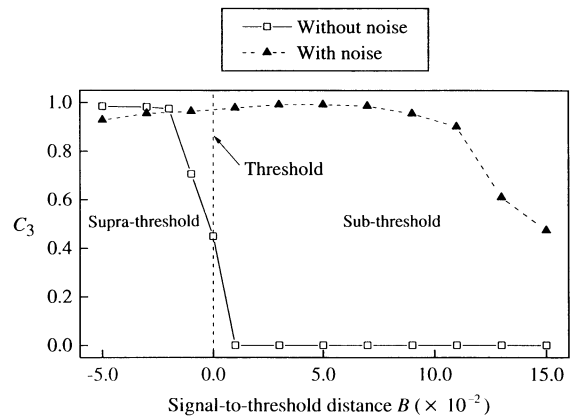


FIG. 3 Values of the normalized power norm  $C_3$  versus signal-to-threshold distance  $B$  for a 1,000-unit summing network without and with fixed levels of independent noise on each of its excitable units. In the latter case, the intensity  $D$  of each unit's input noise was equal to  $1.88 \times 10^{-6}$ . This value was taken from the plateau region in the results for the 1,000-unit summing network in Fig. 2. The values for  $C_3$  were determined using the methods described in Fig. 2 legend. The input signal  $S(t)$  used in Fig. 2 was used for all results presented.

level of independent noise on each unit of such a network can optimally enhance the network's ability to detect a range of sub-threshold signals. This is in contrast to ASR<sup>22</sup> (or SR<sup>15</sup>) in a single excitable unit, which requires the input noise intensity to be systematically modulated as a function of the changing characteristics (for example, variance or signal-to-threshold distance) of the signal to be detected. Importantly, the presence of a fixed level of unit-independent noise also does not significantly affect the ability of a relatively large summing network to detect supra-threshold signals (Fig. 3). With both supra- and sub-threshold signals, the averaging action of the network cancels out the incoherent errors introduced by the noise on each unit. Thus, additive noise reduces the 'effective threshold' of the network (Fig. 3), without significantly degrading the network's ability to detect supra-threshold signals. In this manner, the noise serves to extend the operating range of the overall system.

From a technological standpoint, these novel results suggest that additive noise could be incorporated into the design of a multi-component signal-detection system so as to improve the system's ability to detect weak signals. In addition, this work suggests that the noise intrinsic to each component, which has previously been viewed as a limiting factor for system performance, could be used to improve the sensitivity of the overall system.

Likewise, from a neurophysiological standpoint, these findings suggest a possible functional role for neuronal noise<sup>14,16,18</sup> in sensory systems. It has been speculated that sensory systems may have evolved the capability to take advantage of SR<sup>5,10,12</sup>. However, physiological mechanisms by which the noise on a given sensory neuron could be dynamically modulated as a function of the changing nature of a weak signal (one which would first have to be detected by some component of the nervous system) have not been identified. The present findings indicate that such mechanisms may be unnecessary, and instead constant levels of internal or external noise on each neuron in a sensory system could optimally enhance the overall response of the system to a range of sub-threshold signals, even for conditions wherein the individual responses of the neurons are not optimized. □

Received 5 May; accepted 26 June.

1. Benzi, R., Sutera, S. & Vulpiani, A. *J. Phys.* **A14**, L453–L457 (1981).
2. Nocolis, C. *Tellus* **34**, 1–9 (1982).
3. Benzi, R., Parisi, G., Sutera, A. & Vulpiani, A. *Tellus* **34**, 10–18 (1982).

4. Fauve, S. & Heslot, F. *Phys. Lett.* **A97**, 5–7 (1983).
5. Moss, F., Pierson, D. & O'Gorman, D. *Int. J. Bifurc. Chaos* **4**, 1383–1397 (1994).
6. Wiesenfeld, K. & Moss, F. *Nature* **373**, 33–36 (1995).
7. Jung, P. *Phys. Rep.* **234**, 175–295 (1993).
8. Hibbs, A. D. et al. *J. appl. Phys.* **77**, 2582–2590 (1995).
9. Longtin, A., Bulsara, A. & Moss, F. *Phys. Rev. Lett.* **67**, 656–659 (1991).
10. Bulsara, A., Jacobs, E. W., Zhou, T., Moss, F. & Kiss, L. *J. theor. Biol.* **152**, 531–555 (1991).
11. Douglass, J. K., Wilkens, L., Pantazelou, E. & Moss, F. *Nature* **365**, 337–340 (1993).
12. Moss, F., Douglass, J. K., Wilkens, L., Pierson, D. & Pantazelou, E. *Ann. N.Y. Acad. Sci.* **706**, 26–41 (1993).
13. Longtin, A. *J. statist. Phys.* **70**, 309–327 (1993).
14. Chialvo, D. R. & Apkarian, A. V. *J. statist. Phys.* **70**, 375–391 (1993).
15. Wiesenfeld, K., Pierson, D., Pantazelou, E., Dames, C. & Moss, F. *Phys. Rev. Lett.* **72**, 2125–2129 (1994).
16. Denk, W. & Webb, W. *Phys. Rev. Lett.* **63**, 207–210 (1989).
17. Croner, L. J., Purpura, K. & Kaplan, E. *Proc. natn. Acad. Sci. U.S.A.* **90**, 8128–8130 (1993).
18. Braun, H. A., Wissing, H., Schäfer, K. & Hirsch, M. C. *Nature* **367**, 270–273 (1994).
19. Shepherd, G. M. *Neurobiology*, 2nd edn (Oxford Univ. Press, 1988).
20. Pantazelou, E., Moss, F. & Chialvo, D. in *Noise in Physical Systems and 1/f Fluctuations* (eds Handel, P. H. & Chung, A. L.) 549–552 (Am. Inst. Physics Press, New York, 1993).
21. Knight, B. W. *J. gen. Physiol.* **59**, 734–766 (1972).
22. Collins, J. J., Chow, C. C. & Imhoff, T. T. *Phys. Rev. Lett.* (submitted).
23. Jung, P., Behn, U., Pantazelou, E. & Moss, F. *Phys. Rev.* **A46**, R1709–R1712 (1992).
24. Kiss, L. B. et al. *J. statist. Phys.* **70**, 451–462 (1993).
25. Bulsara, A. R. & Schmeira, G. *Phys. Rev.* **E47**, 3734–3737 (1993).
26. Neiman, A. & Schimansky-Geier, L. *Phys. Lett.* **A197**, 379–386 (1995).
27. Inchiosa, M. E. & Bulsara, A. R. *Phys. Lett.* **A200**, 283–288 (1995).
28. Inchiosa, M. E. & Bulsara, A. R. *Phys. Rev.* **E** (in the press).
29. Inchiosa, M. E., Bulsara, A. R., Lindner, J. F., Meadows, B. K. & Ditto, W. L. in *Proc. 3rd Technical Conf. on Nonlinear Dynamics (Chaos) and Full Spectrum Processing* (Am. Inst. Physics Press, New York, in the press).
30. Lindner, J. F., Meadows, B. K., Ditto, W. L., Inchiosa, M. E. & Bulsara, A. R. *Phys. Rev. Lett.* (in the press).
31. Kiss, L. B. in *Proc. 3rd Technical Conf. on Nonlinear Dynamics (Chaos) and Full Spectrum Processing* (Am. Inst. Physics Press, New York, in the press).
32. Gingl, Z., Kiss, L. & Moss, F. *Europhys. Lett.* **29**, 191–196 (1995).
33. Kramers, H. A. *Physica* **7**, 284–302 (1940).
34. De Luca, C. J., Lefever, R. S., McCue, M. P. & Xenakis, A. P. *J. Physiol.* **329**, 113–128 (1982).
35. Mannella, R. & Paleschi, V. *Phys. Rev.* **A40**, 3381–3386 (1989).

ACKNOWLEDGEMENTS. We thank A. Pavlik for assistance with the preparation of figures. This work was supported by the US National Science Foundation.

## Why gold is the noblest of all the metals

B. Hammer\*† & J. K. Nørskov\*

\* Centre for Atomic-scale Materials Physics, Physics Department, Technical University of Denmark, DK-2800 Lyngby, Denmark

† Joint Research Center for Atom Technology (JRCAT), 1-1-4 Higashi, Tsukuba, Ibaraki 305, Japan

THE unique role that gold plays in society is to a large extent related to the fact that it is the most noble of all metals: it is the least reactive metal towards atoms or molecules at the interface with a gas or a liquid. The inertness of gold does not reflect a general inability to form chemical bonds, however—gold forms very stable alloys with many other metals. To understand the nobleness of gold, we have studied a simple surface reaction, the dissociation of  $H_2$  on the surface of gold and of three other metals (copper, nickel and platinum) that lie close to it in the periodic table. We present self-consistent density-functional calculations of the activation barriers and chemisorption energies which clearly illustrate that nobleness is related to two factors: the degree of filling of the antibonding states on adsorption, and the degree of orbital overlap with the adsorbate. These two factors, which determine both the strength of the adsorbate–metal interaction and the energy barrier for dissociation, operate together to the maximal detriment of adsorbate binding and subsequent reactivity on gold.

In discussing nobleness, we distinguish between the ability of the metal to form and break bonds at the surface, and its ability to form new compounds (such as oxides and carbides) or be dissolved. The latter ability is closely related to the former: to form a compound it is necessary that the metal is able to bond to other atoms, but the formation of a new compound or the dissolution of the metal also involves the breaking of the metal–

metal bonds. We first consider the surface reactivity of the metals and then comment on the consequences for the more general ‘bulk-nobleness’.

Figure 1 summarizes the calculated reaction energetics for  $H_2$  on the (111) surface of the four metals, Ni, Cu, Pt and Au. It can be seen that  $H_2$  dissociation is activated on Cu and Au, and non-activated on Ni and Pt, in complete agreement with experimental evidence<sup>1,8</sup> and previous calculations where available (Ni, Cu)<sup>9,13</sup>. It is also seen that Au stands out as having both the highest barrier for dissociation and the least stable chemisorption state. The lack of reactivity of gold is thus clearly borne out by the calculations.

As a starting point for analysing the repulsive hydrogen–gold interaction we consider in Fig. 2a the simple two-level interaction problem. When the electronic states of two atoms overlap, quantum mechanics dictates that they be orthogonal to each other. This drives up the energy and leads to so-called Pauli repulsion. However, the overlapping states will also hybridize and form bonding and antibonding states. If only the bonding state becomes occupied, the hybridization effect will be attractive and will counteract the orthogonalization energy cost. If, on the other hand, both the bonding and antibonding state become occupied no hybridization energy is gained and the orthogonalization energy cost prevails.

This simple two-level problem can be transferred to the case of hydrogen chemisorption on the transition-metal and noble-metal surfaces. Here the adsorbate–surface interaction is most conveniently considered in two steps<sup>14–16</sup>. First, the interaction of the hydrogen 1s state with the metal 4s (Ni and Cu) or 6s (Pt and Au) band leads to a deep-lying filled bonding state and an empty antibonding state. This interaction is therefore attractive and, as the *s*–*s* coupling matrix element varies little for the metals considered, the attraction should be about the same for all four surfaces<sup>17,18</sup>. Then follows the interaction of the bonding state with the metal *d* states. As illustrated in Fig. 2b this results in an extra bonding shift of the hydrogen-induced state, but also

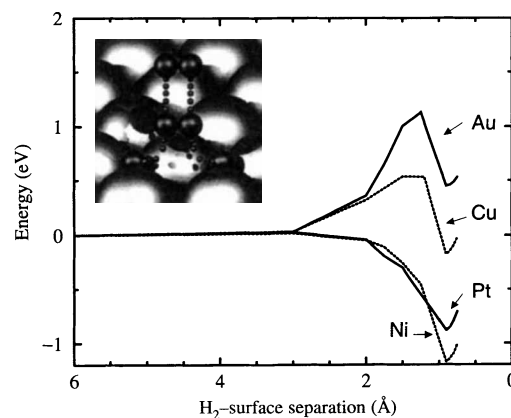


FIG. 1 Main figure, the calculated energy along the minimum-energy reaction path for  $H_2$  dissociating on the (111) surface of Ni, Cu, Pt and Au. The  $H_2$ –surface separation is the height of the molecular centre of mass above the plane of the surface atoms. For each height, the H–H bond length has been allowed to relax to give the lowest-energy configuration, and in a similar way the configuration of the molecule relative to the surface unit cell has been allowed to relax on the way towards the surface. Inset, the calculated reaction path for  $H_2$  dissociating on the Au(111) surface. The reaction paths on the other metals also involve an orientation of the molecular axis parallel to the surface. The calculations are done for a super-cell geometry with one  $H_2$  molecule per  $\sqrt{3} \times \sqrt{3}$  surface unit cell on one side of metal slabs consisting of four atomic (111) layers. The total energies are calculated from density-functional theory<sup>20</sup> describing exchange and correlation effects in the local density approximation augmented by non-local corrections in the so-called generalized gradient approximation (GGA)<sup>21</sup>.